Magnetic-field behavior of the spin-density-wave state in $(TMTSF)_2AsF_6$

J. L. Musfeldt* and M. Poirier
Centre de Recherches en Physique du Solide, Département de Physique, Université de Sherbrooke, Sherbrooke, Québec, Canada J1K 2R1

P. Batail and C. Lenoir
Laboratoire de Physique des Solides, Université Paris-Sud, 91405 Orsay, France
(Received 12 January 1995)

We report the 16.5 GHz microwave response of single crystal samples of $(TMTSF)_2AsF_6$ at temperatures from 1.7–20 K as a function of external magnetic field. With the field applied along the hard (c^*) axis direction, striking changes are observed below T_c in the microwave dielectric constant and conductivity, which are similar to (but more clear than) those reported in the PF_6 salt. Following small changes in the low-temperature dielectric response, we are able to resolve the field dependence of the 3.5 and 1.9 K condensate phase boundaries. For the field applied along the chain direction, no changes are observed. Emphasis is placed upon the analysis of the H-T diagram ($H \| c^*$) and the series of subphases within the spin-density-wave manifold.

I. INTRODUCTION

Studies of the $(TMTSF)_2X$ family of low dimensional synthetic metals have attracted a great deal of interest recently.[1–3] These organic charge transfer salts exhibit a rich plethora of exotic phenomena,[4] including metallic behavior, spin-density-wave ground state, field induced spin-density waves, and superconductivity. The ability to manipulate the dimensionality (and select the ground state) makes the Bechgaard family of salts very attractive compounds to study. The salts with octahedral counterions ($X = PF_6$, AsF_6, SbF_6, or TaF_6) are prototypes in this family of organic materials due to the formation of the spin-density-wave (SDW) ground state. This broken symmetry state is brought about by repulsive electron-electron interactions and Fermi surface nesting considerations, which are responsible for the destruction of the metallic conductivity and the stabilization of an antiferromagnetic state below 12 K. The strong anisotropy in the low temperature magnetic susceptibility[5] combined with the absence of structural distortion at T_c (Refs. 6,7) was crucial in distinguishing the broken symmetry ground state in TMTSF compounds from that brought about by electronic or spin-Peierls processes.[8–10]

In the high temperature phase, the electromagnetic response of a representative salt such as $(TMTSF)_2PF_6$ consists of a Drude relaxation (as expected for "metallic" samples) and a gaplike structure in the far-infrared.[11–14] Below T_c, the frequency dependent conductivity has contributions from internal deformations and the pinning mode of the density wave, as well as the temperature independent far-infrared feature (which remains unchanged).[11–13,15] Because the nature of the collective mode dominates the low temperature phase dynamics in these systems, microwave and millimeter wave dielectric studies are extremely important for studying the density wave state in Bechgaard salts. The major results accrued over the past decade[11,12,15–22] can be summarized as follows. Below T_c, the excess conductivity observed at ac frequencies has been attributed to the current carrying capacity of the collective mode. The presence of this mode results in a strongly frequency dependent dielectric response.[11,16,17] At the same time, the highly polarizable nature of the ground state results in a large dielectric constant (on the order of 10^5) at these frequencies.[25] More recently, we reported high precision microwave dielectric measurements on the spin-density-wave state of $(TMTSF)_2PF_6$ and $(TMTSF)_2AsF_6$.[23,24] In addition to signalling the opening of the SDW gap at 12 K, features in ϵ_1 and σ_1 seem to announce changes in the condensate behavior below T_c. We have attempted to correlate structures in the dielectric response with changes in other independent physical properties. The strong magnetic field dependence of the 3.5 K feature is curious and is the subject of continuing investigations. The dielectric constant continues to rise at lower frequency and has been estimated to reach a limiting (zero frequency) value of $\approx 2 \times 10^9$.[25] The extraordinarily high value of ϵ_1 has been attributed to the easily polarizable *internal* ($q \neq 0$) modes of the SDW condensate.[25] More recent dielectric studies on $(TMTSF)_2PF_6$ at radio frequencies[26] display a very low temperature relaxation that is not well described by the typical activated behavior. The shift in position with frequency is attributed to a glassy transition with a limiting value of ≈ 2 K. Low energy dielectric studies have also been carried out on a series of TMTSF alloys $[(TMTSF)_2(AsF_6)_{1-x}(SbF_6)_{1-x}]$, where the disorder introduced by the composite nature of the samples is used to control the SDW pinning.[27,28]

NMR measurements have also commanded sustained interest during the past decade because they represent a powerful technique for probing the nature of the broken symmetry ground state in TMTSF-based organics.[29–37] From changes in the spin-lattice relaxation time (T_1^{-1}) at ambient pressure, instabilities are observed near 12.1, 3.5, and 1.9 K.[34] This divides the low-temperature phase diagram into three regimes, usually labeled SDW 1, SDW 2, and SDW 3, respectively. The pressure dependence of these subphase boundaries shows that SDW 3 competes directly with the superconducting ground state.[34] Less work has been devoted to mapping out the magnetic field dependence of the sub-

0163-1829/95/52(22)/15983(9)/$06.00

phases within the SDW manifold. In a recent study, the sharp falloff in T_1^{-1} near 3.5 K has been shown to display a weak magnetic field dependence between 0.25 and 1.25 T.[31] This structure has been attributed to the slowing down of phason dynamics.[29,31]

Numerous physical property measurements have been used to characterize the low-temperature phase and establish legitimacy for the instabilities observed by NMR. The thermodynamic studies provide the strongest indication that the metal → insulator transition and the aforementioned changes in condensate behavior (at 3.5 and 1.9 K) are related to true phase transitions.[38,39] However, in contrast to the 12 K transition, both specific heat and elasticity experiments show the 3.5 K feature to be weakly coupled to the underlying lattice.[39,40] There is evidence for a kinetic contribution to the 3.5 K transition as well.[26] The low frequency dielectric measurements point to a critical slowing down behavior (due to a glassy transition) as the origin for the changing phason dynamics in this regime,[26,41] with the large domain size being responsible for the strongly non-Arrhenius relaxation behavior. A strong increase in the threshold field is also observed near 3.5 K.[42] The disappearance of the Shubnikov–de Haas magnetoresistance oscillations suggests a modification of the Fermi surface near 3.5 K as well.[43]

In order to gain additional insight into the nature of the 12 K phase transition and the underlying cascade of instabilities, we have investigated the 16.5 GHz microwave response of $(TMTSF)_2AsF_6$ as a function of temperature and applied magnetic field. Microwave dielectric studies are very important for studying the broken symmetry ground state in the Bechgaard salts because the collective mode resonates in this energy regime and has been shown to dominate the low-temperature dynamics. These particular studies were motivated by the current evidence for different SDW states below T_c, and the expectation that the various SDW states should respond differently in a magnetic field. The strong magnetic field effects ($H \parallel c^*$) observed in ϵ_1 and ϵ_2 of the PF_6 salt are even more clear in the AsF_6 compound.[24] This has allowed us to follow several weak features and generate a diagram which describes the H-T behavior of the SDW condensate at low temperatures and magnetic fields. Our discussion concentrates on the relationship between the low-temperature dielectric features and similar anomalies in other physical properties. One of the main goals of this paper is to present a detailed explanation of the data which has allowed us to generate the H-T diagram, although the diagram itself has been published previously.[24] We also take this opportunity to summarize our results for both the AsF_6 and PF_6 systems.

II. EXPERIMENT

A. Sample preparation

Single crystals of $(TMTSF)_2AsF_6$ were grown by standard electrochemical methods. The shiny black needles had typical dimensions of $\approx 0.25 \times 0.0125 \times 0.0043$ cm, which is significantly thinner than the PF_6 samples used in the previous investigation.[23] Our method of sample handling and for fixing the crystal in the intended orientation has been described elsewhere.[23] The samples were cooled slowly to 4 K to prevent microcracking and outright breakage, which was evidenced by a sharp increase in the resonance frequency. Unnecessary thermal cycling was avoided.

B. Microwave cavity measurements

We used a microwave cavity perturbation technique to measure the complex dielectric function $\epsilon^* = \epsilon_1 + i\epsilon_2$ of a $(TMTSF)_2AsF_6$ single crystal as a function of temperature (in the range 1.7–20 K) and external magnetic field (0–7 T); here, ϵ_1 and ϵ_2 are the dielectric constant and the dielectric loss, respectively. The conductivity, σ_1, is related to the lossy response as $\epsilon_0 \epsilon_2 \omega$. The experiment was conducted in a rectangular copper cavity operated at 16.5 GHz in the TE_{102} transmission mode. The two quantities of interest in this experiment are the perturbation of the resonance frequency ($\delta\omega/\omega$) and the quality factor [$\Delta(1/2Q)$] of the cavity upon insertion of the sample at the electric field maximum ($H_{ac}=0$). The reference is, of course, the empty cavity. All measurements were done with the electric field vector parallel to the TMTSF chain axis direction. Using our apparatus, frequency and bandwidth changes can be measured with a sensitivity of better than 1 part in 10^{-7}; 5 mK precision was achieved in temperature control.

Our specific measurements can be summarized as follows: we have made both temperature and magnetic-field sweeps of the two experimental parameters, concentrating on the 1.7–7 K and 0–3 T range. A few runs were made to higher temperature and field. For the temperature sweeps, $\delta\omega/\omega$ and $\Delta(1/2Q)$ were measured at intervals of 0.15 K at a rate of 0.6 K/min; a static external magnetic field could be applied along the hard (c^*) or chain (a) axis direction of the crystal. The field sweeps were taken at ≈0.05 T/min at constant temperature (±0.15 K). In certain runs, a glitch is observed near 0.2 T, which we attribute to Eddy heating.

C. Data analysis

The results were analyzed within the framework of the quasistatic approximation,[46] where the real and imaginary parts of the dielectric function are given as

$$\epsilon_1 = 1 - \frac{\left[\frac{\delta\omega}{\omega}\left(\frac{\delta\omega}{\omega}+\frac{\alpha}{N}\right)+\left(\Delta\frac{1}{2Q}\right)^2\right]}{N\left[\left(\frac{\delta\omega}{\omega}+\frac{\alpha}{N}\right)^2+\left(\Delta\frac{1}{2Q}\right)^2\right]} \tag{1}$$

and

$$\epsilon_2 = \left(\frac{\alpha}{N^2}\right)\frac{\left(\Delta\frac{1}{2Q}\right)}{\left[\left(\frac{\delta\omega}{\omega}+\frac{\alpha}{N}\right)^2+\left(\Delta\frac{1}{2Q}\right)^2\right]}. \tag{2}$$

Here, N is the depolarization factor along the direction of the electric field and α is the cavity filling factor. These parameters are determined from a knowledge of the sample and cavity geometry.[47] Although the quasistatic approximation is derived strictly for situations where the field is uniform over the sample, this constraint can be relaxed somewhat for practical use. In the case of our samples, 2× the penetration depth is on the order of the sample thickness (≈43 μm),

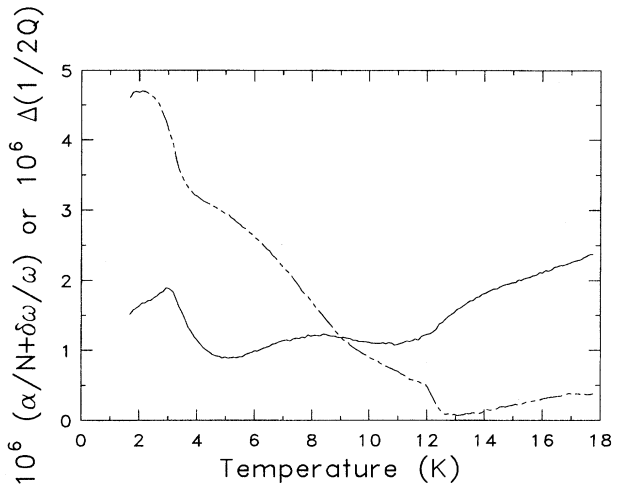

FIG. 1. $\Delta(1/2Q)$ (solid line) and $(\alpha/N + \delta\omega/\omega)$ (double-dashed line) as a function of temperature at 16.5 GHz.

suggesting that the field is *nearly* uniform over the crystal and that the quasistatic approximation is appropriate here.

To illustrate the size of the two important contributions in Eqs. (1) and (2), some typical zero field data are displayed in Fig. 1. The experimental frequency shift has been corrected for the thermal expansion, as described previously.[23] The term $(\alpha/N + \delta\omega/\omega)$ is finite in the normal state and climbs steeply in the SDW phase, eventually growing to dominate the lossy term. Although measurements on certain AsF_6 crystals resulted in raw data curves which were similar to those reported previously for the PF_6 salt,[23] we have *specifically chosen* to present data from an unusual sample for which $\delta\omega/\omega$ and $\Delta(1/2Q)$ *appear* drastically different from the norm. (For instance, in this sample, evidence for the metal $\rightarrow$ insulator transition appears primarily on the frequency shift.) Our goal is to illustrate that neither $\delta\omega/\omega$ nor $\Delta(1/2Q)$ are general features of the AsF_6 response: they must be combined to calculate ϵ_1 and σ_1.

Our method of analysis differs from the usual treatment of microwave cavity data on the Bechgaard salts,[11,12,15–21] where it is customary to relate the real part of the surface impedance to the "microwave resistivity" as

$$\rho = \frac{2R_s^2}{\mu_0 \omega}. \tag{3}$$

Here, R_s is the surface resistance (which is determined solely from the lossy response), μ_0 is the permeability of free space, and ω is the angular frequency. Neglect of the surface reactance term, X_s, is generally a practical consideration, resulting from the difficulty of an accurate measurement of the frequency shift.[11,15,20] Because we are not limited by constraints on the measurement precision of $\delta\omega/\omega$, we can test whether it should be included in the analysis. As discussed in the following paragraph, we believe it should.

The "microwave resistivity" framework is very useful when considering highly conducting samples of sufficient thickness (such that the penetration depth $\ll$ than the sample thickness), but one must demonstrate that $X_s = R_s$ in order to apply the approximation with confidence.[23] For our samples, R_s and X_s cannot be placed in perfect coincidence, even in a limited temperature range near 12 K (Fig. 2), demonstrating the broad inapplicability of the "microwave resistivity" approximation to these samples. Thus the frequency shift will have a unique and important contribution to the dielectric response. This contribution is especially critical below T_c. A similar result could also be anticipated from sample thickness considerations or by noting the clear change in $\delta\omega/\omega$ at T_c.

D. Generation of the *H-T* diagram

We constructed the 16.5 GHz *H-T* diagram for $(TMTSF)_2AsF_6$ following small anomalies in ϵ_1 and σ_1 which seem to define changes in condensate behavior. We believe that these low-temperature features can be attributed to changes in the density wave dynamics because the dc conductivity (which measures the quasiparticle contribution) is structureless below T_c.[44] That these features are observed well below T_c (where quasiparticle effects are expected to be frozen out) provides additional support for our procedure. However, Hall mobility measurements indicate a possible coupling between the density wave and normal carriers in this regime,[49] and such a possibility should not be neglected in further analysis. Motivated by the fact that ϵ_1 might be expected to show the largest variation at a phase transition,[50] we have taken the maximum of $\partial\epsilon_1/\partial T$ (or $\partial\epsilon_1/\partial H$ in the case of field sweeps) as the signature of the transition. Other reasonable choices (such as the maximum in σ_1 or $\partial\sigma_1/\partial T$) result in a qualitatively similar diagram, although the resulting phase boundary temperatures are slightly offset. Similar changes in condensate behavior can also be surmised from examination of either $\delta\omega/\omega$ or $\Delta(1/2Q)$ alone, although an effort was made not to rely too heavily on the individual quantities because the correct dielectric response is provided by a *mixture* of both contributions. Error bars on the points determined by temperature sweep are ± 0.2 K in

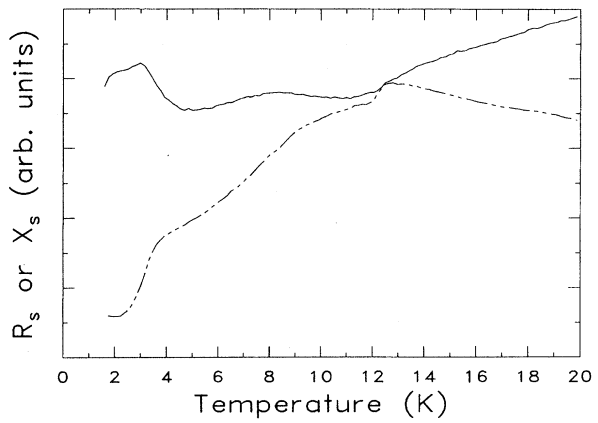

FIG. 2. The surface resistance (solid line) and the surface reactance (double-dashed line) of $(TMTSF)_2AsF_6$ as a function of temperature at 16.5 GHz. The lack of long-range coincidence of R_s and X_s indicates the inapplicability of the "microwave resistivity" approximation to our samples.

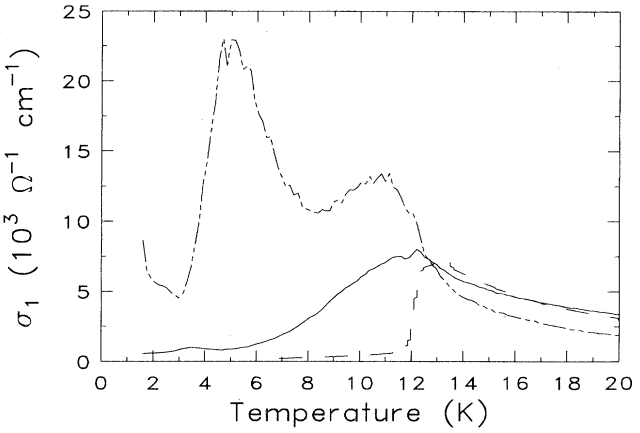

FIG. 3. 16.5 GHz conductivity of $(TMTSF)_2AsF_6$ calculated within the quasi-static approximation (solid line) and the "microwave resistivity" approximation (double-dashed line) as a function of temperature. The dc conductivity (dashed line) is also shown. Note that the level of $1/\rho_{micro}$ and σ_{dc} has been normalized to our data at 12 K.

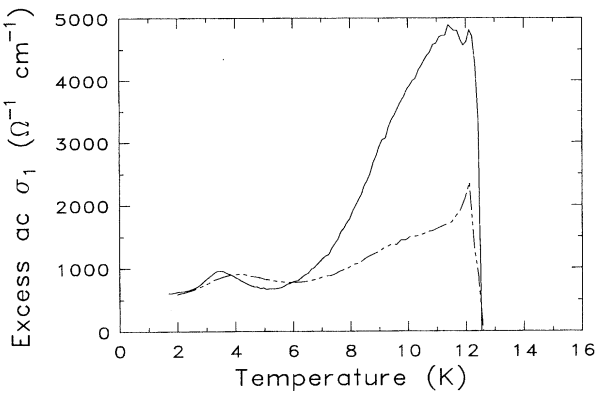

FIG. 4. Excess conductivity of $(TMTSF)_2AsF_6$ (solid line) and $(TMTSF)_2PF_6$ (double-dashed line) as a function of temperature at zero field and 16.5 GHz. The cusp near 12 K is due to slope mismatches between σ_{ac} and σ_{dc}.

the "worst cases," whereas for the "best cases" (when the transition is sharp), error bars are $\approx \pm 0.05$ K. The derivatives of ϵ_1 are also less reliable near the low-temperature sweep limit. Consequently, the points below 2 K and 0.5 T on the H-T diagram represent our "best estimate" of the position of the dielectric anomaly taken directly from the upturn in ϵ_1 (rather than by the derivative method). Significantly greater noise was obtained on the field sweep runs; that, combined with the difficulty in distinguishing a transition based upon very small differences in ϵ_1, lead to significantly increased error bars on these points (± 0.2 T and ± 0.1 K).

III. RESULTS

A. Zero field measurements

Figure 3 displays the zero field temperature profile of the 16.5 GHz conductivity in $(TMTSF)_2AsF_6$. The microwave conductivity is high in the normal state and in reasonable agreement with the thermal dependence of the dc conductivity. σ_1 decreases below 12 K, but more gradually than in the PF_6 salt.[23] This observation is in agreement with recent dc conductivity results.[48] A local maximum in σ_1 is observed near 3.5 K, which is absent when $\delta\omega/\omega$ is neglected from the analysis. A similar feature was observed in the PF_6 compound.[23]

Considering the important role that microwave dielectric studies have played in discerning the unique properties of the broken symmetry ground state in TMTSF systems during the past decade, it is useful to compare our conductivity data with earlier results based upon the "microwave resistivity" approach and to clearly motivate what prompts us to engage in a different method of analysis. To this end, we have calculated the "microwave resistivity" [which depends solely on the lossy response as shown in Eq. (3)] in the manner of the previous authors[11,12,15–21] and plotted it ($\sigma_{micro} = 1/\rho_{micro}$) alongside our data and the scaled dc conductivity of Traetteberg *et al.*[51] in Fig. 3. Neglect of the frequency shift in the data analysis substantially alters the low-temperature phase conductivity profile. The difference between the various curves is even more striking than that reported earlier for the PF_6 salt.[23]

Subtraction of the dc conductivity (which is related to the quasiparticle contribution) from the microwave conductivity leaves us with a better measure of the excess ac conductivity and a clearer picture of the collective mode contribution to the transport below T_c. Such a separation is based upon the assumption of a "two-component" (free carrier + condensate) model and its applicability to the low-temperature dielectric properties of the Bechgaard salts. It also assumes the quasiparticle contribution is frequency independent in this range, and it ignores any interaction between free carriers and the density wave. The dc conductivity was obtained from the literature[51] and normalized to our data above T_c. Naturally, it would be preferable to use the dc response from the same sample, but we are not equipped to make these measurements in our lab. In addition, it is difficult to obtain a "universal" dc conductivity from the literature, so the subtraction is intended to provide only *a qualitative* indication of this difference. We display σ_{ac}-σ_{dc} in Fig. 4. Qualitatively similar behavior is observed for both the AsF_6 and PF_6 salts.

An additional advantage of treating the data based upon Eqs. (1) and (2) (as opposed to the "microwave resistivity" approximation) is the accessibility of the real part of ϵ^*. We display the zero field 16.5 GHz dielectric constant of $(TMTSF)_2AsF_6$ (together with the temperature derivative of ϵ_1) in Fig. 5. As expected, ϵ_1 is large ($\approx 3 \times 10^5$), consistent with the highly polarizable nature of the condensate at microwave frequencies and in reasonable agreement with that obtained for the PF_6 salt.[23] In the low-temperature phase, ϵ_1 displays a downward slope at intermediate temperatures, with an inflection near 8 K, a sharp drop near 3.5 K (concomitant with a local maximum in the lossy response), and a slight upturn at lower temperatures ($\approx$1.8 K). As for the PF_6 salt, ϵ_1 seems to be accessible in the normal state, and we attribute the sharp increase of ϵ_1 at 12 K (T_c) to the opening of the spin-wave gap. The shape of ϵ_1 above 12 K is probably more realistic than that reported for

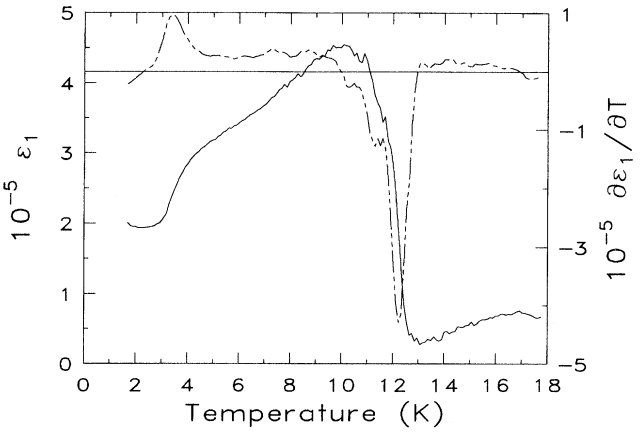

FIG. 5. Solid line: 16.5 GHz dielectric constant of $(TMTSF)_2AsF_6$ as a function of temperature taken at zero magnetic field. Double-dashed line: $\partial\epsilon_1/\partial T$, illustrating how points in Fig. 10 were determined.

the PF_6 compound.[23] However, significant errors in this quantity are likely to be present above T_c (see Ref. 23 for a discussion), and ϵ_1 should not be considered reliable there.

B. Magnetic-field effects

In this section, we present the change in frequency and bandwidth, as well as the dielectric response, as a function of temperature and magnetic field for $(TMTSF)_2AsF_6$ at 16.5 GHz. Although we have studied two separate configurations ($H\|c^*$ and $H\|a$), we concentrate primarily on the data taken in the presence of the transverse field.

1. H along the hard axis direction

The experimental frequency shift and the change in bandwidth of $(TMTSF)_2AsF_6$ as a function of external magnetic field applied along the hard axis direction (c^*) of the crystal are displayed in the upper and lower panels of Fig. 6, respectively. The clear correlations in the data emphasize the fact that $\delta\omega/\omega$ and $\Delta(1/2Q)$ are not independent quantities.

There are three main features of interest in Fig. 6. At zero field, the metal→insulator transition is observed at ≈12.1 K. T_c increases to ≈12.2 K at 3 T. While the transition is evidenced by a sharp change in $\delta\omega/\omega$, it is not clearly observed on the bandwidth for this sample. The second structure presents itself as a local depression in the frequency shift and as a maximum on the bandwidth near 3.5 K. At low applied field, this feature broadens and moves to higher temperature with increasing field. Similar behavior is observed in the PF_6 compound.[23] Evidence for a third structure appears near 2 K in the raw data; it displays weaker field dependence than the 3.5 K feature.

The 16.5 GHz dielectric constant as a function of temperature for various magnetic fields is shown in Fig. 7. The strongest changes are observed at low temperature, where curves taken at different fields illustrate the progressive changes in ϵ_1 with $H \parallel c^*$. To highlight the low-temperature/low-field response, we also display a three-dimensional

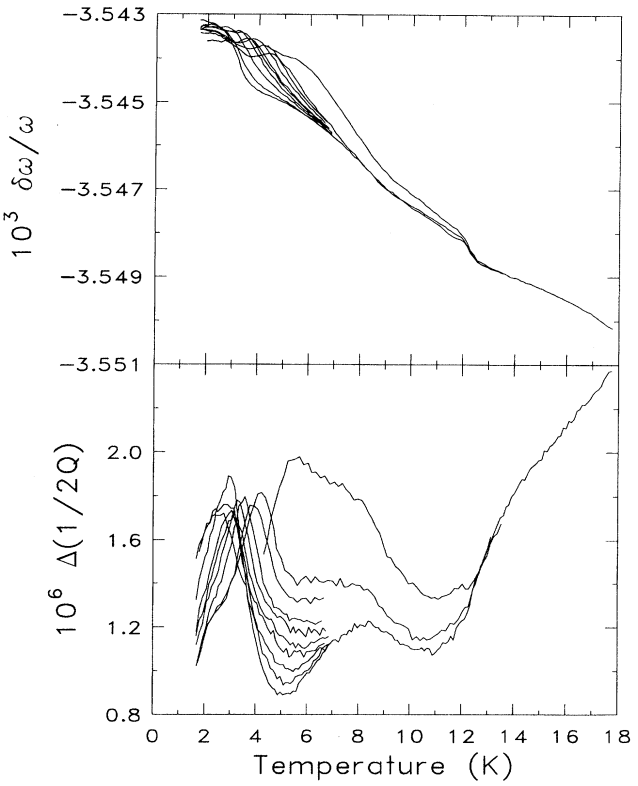

FIG. 6. Upper panel: experimental $\delta\omega/\omega$ as a function of temperature and magnetic field at 16.5 GHz; lower panel: $\Delta(1/2Q)$ as a function of temperature and magnetic field at 16.5 GHz. The external magnetic field is applied along the hard axis (c^*) direction. Selected field strengths: H = 0, 0.2, 0.5, 0.8, 1.0, 1.4, 1.8, 2.5, 3.0, 7 T. Curves change monotonically with increasing H.

close-up view of the H-T behavior of the 16.5 GHz dielectric constant in Fig. 8. The aforementioned local depression in $\delta\omega/\omega$ manifests itself as a rapid decrease in ϵ_1 near 3.5 K. With increasing field above ≈0.5 T, the sharp drop in ϵ_1 becomes less prominent and moves to higher temperature, tracking the local maximum in σ_1. The width of the anomaly increases considerably as well, indicating a reduced sample polarizability in the presence of a field. As expected from the two experimental quantities in Fig. 6, a second feature becomes evident in ϵ_1 near 2 K and moves to higher temperature with increasing H. At 7 T, the second structure is centered near 6 K, in excellent agreement with results on the PF_6 salt.[23]

The 16.5 GHz conductivity for $(TMTSF)_2AsF_6$ displays complementary behavior as a function of H and T. In the absence of the magnetic field, the 3–4.5 K regime is characterized by a small local increase in the conductivity. Above 0.5 T, this feature broadens, weakens, and moves to higher temperature, behavior which (in combination with the aforementioned behavior of ϵ_1) seems to define a phase boundary between SDW 1 and SDW 2.[34] The local maximum in σ_1 is difficult to discern by 3 T. In the PF_6 sample, the analogous feature weakens near 4 T and is completely disappeared at 10 T.[23] In a similar manner, the 2 K feature is present as a small

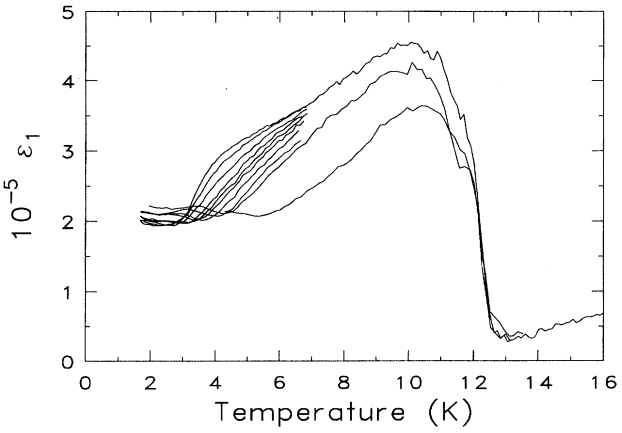

FIG. 7. 16.5 GHz dielectric constant of $(TMTSF)_2AsF_6$ as a function of temperature and magnetic field. The external magnetic field is applied along the hard axis (c^*) direction. Selected field strengths: H = 0, 0.2, 0.5, 0.8, 1.0, 1.4, 1.8, 2.5, 3.0, 7.0 T. Curves change monotonically with increasing H.

downturn at low fields and "grows in" clearly above $\approx$ 0.5 T and moves to higher temperature with increasing field. It displays good amplitude at stronger fields (up to 7 T).

Since one purpose of this paper is to compare recent microwave dielectric results on TMTSF-based SDW systems, it is important to note that the structure near 2 K in the AsF_6 salt also seems to appear very weakly in the PF_6 compound, although it was not reported in Ref. 23. Careful derivatives of the temperature sweep data do manage to resolve similar behavior as described above, although it is not at all obvious, and it is easily missed without the benefit of comparison to the AsF_6 salt.

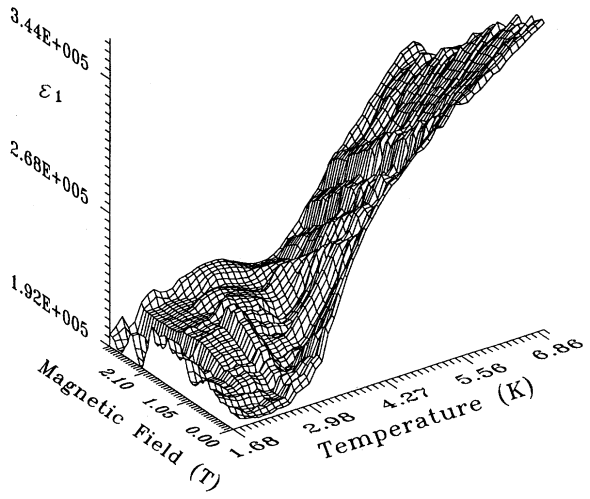

FIG. 8. Close-up three-dimensional plot of the 16.5 GHz dielectric constant of $(TMTSF)_2AsF_6$ as a function of temperature (1–7 K) and magnetic field (0–3 T). The external magnetic field is applied along the hard axis (c^*) direction.

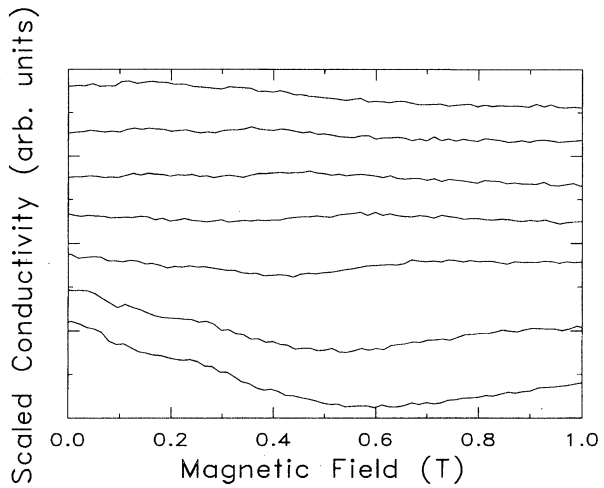

FIG. 9. 16.5 GHz conductivity of $(TMTSF)_2AsF_6$ as a function of magnetic field ($H \parallel c^*$) at constant temperature. From top to bottom, the data are taken at 2.06, 2.24, 2.42, 2.61, 2.82, 3.11, and 3.35 K. For clarity, the curves have been shifted by an arbitrary constant.

We show the 16.5 GHz conductivity as a function of applied magnetic field at various temperatures below the glassy transition in Fig. 9. A weak structure in σ_1 near 0.5 T seems to provide evidence for a subtle change in condensate behavior within SDW 2. As might be expected, ϵ_1 displays a complementary change in the 0.5 T field range. The possible origin of this unexpected regime is discussed in more detail elsewhere.[24]

The H-T diagram for the condensate behavior of $(TMTSF)_2AsF_6$ at 16.5 GHz (obtained for $H \| c^*$) is shown in Fig. 10. As discussed in Sec. II D, these points were determined using derivatives of ϵ_1 to locate changes in condensate behavior. For comparison, we have also included some data taken on the PF_6 salt: the maximum of T_1^{-1} taken at different applied fields ($H \| c^*$) from the NMR study of Clark *et al.*[31] and the lattice specific heat anomalies of Lasjaunias *et al.*[26] The zero field condensate boundaries are observed at $\approx$12.12, $\approx$3.40, and $\approx$1.85 K. These values are in excellent agreement with the anomalies observed in the lattice specific heat measurements.[26]

As shown in Fig. 10, the condensate boundaries move to higher temperature and broaden slightly with increasing magnetic field. The 3.5 K boundary weakens significantly with applied field as well. Similar behavior for the SDW 1$\rightarrow$SDW 2 line can be inferred from the NMR relaxation time data of Clark *et al.*[31] Additional NMR data[32,34] was disqualified from appearing in our plot because the direction of the applied magnetic field was either not along c^* or unknown. The weak 0.5 T boundary within SDW 2 (obtained from the data in Fig. 9) is also indicated.

Finally, we mention that, based upon following the field dependence of a much weaker inflection in ϵ_1, we find evidence for a small change in the SDW condensate behavior in both the AsF_6 and PF_6 salts near 8 K. The position of this anomaly is nearly field independent, and it seems to disap-

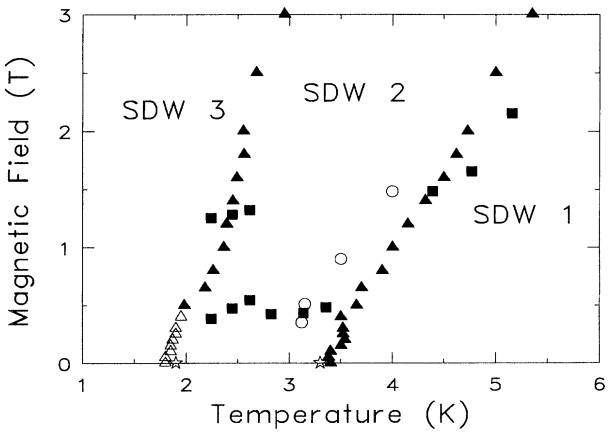

FIG. 10. The H-T behavior of the SDW condensate of $(TMTSF)_2AsF_6$ at 16.5 GHz. The external magnetic field is applied along the hard axis (c^*) direction. Filled triangles: position of dielectric anomaly as determined by temperature sweep at constant field; filled squares: position of dielectric anomaly as determined by magnetic-field sweep at constant temperature; open triangles: position of the low-temperature/low-field dielectric anomaly as *estimated* from temperature sweeps at constant fields; open circles: NMR data of Clark *et al.* (Ref. 31); open stars: specific heat data of Lasjaunias *et al.* (Ref. 26). Note that the data in Refs. 31 and 26 were obtained on the PF_6 salt.

pear above 4 T for $H \parallel c^*$. Early static susceptibility studies[45] also suggested a transition in this temperature range, although the observation received scant attention. More recent experiments have detected a decrease in the nonlinear conductivity between 6 and 9 K;[44] however, the lack of magnetic field dependence in σ_{SDW}/σ_n seems to argue against any direct correlation between the two measurements.

2. *H along the chain axis*

No significant magnetic-field dependence of the raw data is observed when the external field was applied along the TMTSF chain direction. Thus no field dependence ($H \parallel a$) is obtained in either σ_1 or ϵ_1. That the magnetic field fails to induce additional localization effects is due to the strong anisotropy in the band structure.[3] A similar result was obtained for the PF_6 salt.[23] For the external magnetic field in this configuration, the H-T diagram consists of vertical lines which define condensate phase boundaries near 1.85, 3.4, and 12 K. No 0.5 T anomaly was observed within SDW 2 for $H \parallel a$. A weak line would also be drawn near 8 K, defining a less-clear change in condensate behavior.[45] Such an H-T diagram is obviously less interesting than that reported for the $H \parallel c^*$ case.

IV. DISCUSSION

Several aspects of our data for the PF_6 and AsF_6 salts demonstrate that quasiparticle effects dominate the dielectric response in the transition regime. For example, both the weak increase in T_c with applied field and the sharp change in ϵ_1 at 12 K (due to the opening of a spin-wave gap) are expected within the "Fermi nesting" framework.[52–56] However, the role of the free carriers below T_c is less clear. Quasiparticles likely contribute to the low temperature conductivity in a modest way due to imperfect nesting, which causes small regions of phase space to remain gapless.[52]

To quantify various contributions to the conductivity below T_c, we have calculated σ_{ac}-σ_{dc} for both the AsF_6 and PF_6 salts (Fig. 4). Whereas the low-temperature features are similar in both cases, the AsF_6 salt displays a larger "excess conductivity" directly below T_c than does the PF_6 compound. We discuss this result from a "purely quasiparticle" and a "purely condensate" point of view, although it is important to note that such a subtraction may not be valid near T_c and that the results of Fig. 4 may simply reflect the different electronic temperatures as a function of frequency.

From a "purely quasiparticle" point of view, non-nested carriers hopping over a small gap[57] may contribute significantly to the "excess ac conductivity" below 12 K. Thus the curves in Fig. 4 could be interpreted in terms of poorer nesting properties for the AsF_6 salt (as compared with the PF_6 compound). The conductivity due to such a free carrier contribution is expected to decrease with temperature as the gap widens and the remaining "non-nested" carriers freeze out.[11] From a "purely condensate" point of view, the larger "excess ac conductivity" near 10.5 K may reflect a different pinning frequency or a substantially different defect concentration in the AsF_6 compound. The larger threshold field for the AsF_6 salt (as compared to the PF_6 salt) recently reported in Ref. 48 seems to support this hypothesis. (Here, we assume that our 16.5 GHz probe frequency is larger than the center frequency of the collective mode.[1]) An increase in the pinning frequency with decreasing temperature[11,58] could also explain the falloff of the data in Fig. 4. However, it is difficult to fully ascribe the "excess ac conductivity" to condensate effects as the frequency dependence of the quasiparticle conductivity is unknown and the nesting at 12 K is imperfect. Strong interactions or impurity effects can also cause a breakdown of the two-component picture. Clearly, it will not be straightforward to discriminate between quasiparticle and condensate effects in the temperature regime near T_c.

In contrast to the behavior near T_c, the 3.5 K decrease in ϵ_1 (and the corresponding local maximum in σ_1) is probably unrelated to quasiparticle effects, as it occurs far from T_c where free carrier effects are mostly frozen out. That the dc conductivity is featureless in the low-temperature phase provides additional support for this supposition,[44] although a complex interaction between normal and condensate processes cannot be ruled out.[49] Previously, it was suggested that the sharp drop in the dielectric constant near 3.5 K in the PF_6 compound may be a signature of changing condensate behavior.[23] Characterization of the dielectric response in the AsF_6 salt,[24] combined with the recent annealing and kinetic studies by several French authors,[26,41] indicates that the SDW 1 $\rightarrow$ SDW 2 transition is driven by glassy dynamics. An increase in the threshhold field near T_g also indicates a possible change in the density wave dynamics.[42] The structure in the dielectric response near 2 K also seems unrelated to quasiparticle effects.

The dielectric constant displays a sharp drop at the glass transition temperature, T_g, due to the reduced sample polar-

izability sensed by our fixed-frequency experiments as the phason dynamics slow. Within the framework of Adam and Gibbs for a relaxational transition,[61] the reduced sample polarization at T_g is accompanied by a diverging coherence length, ξ_c.[41] Here, ξ_c defines the scale over which long-range spatial correlations take place.[41,61] For the PF_6 salt, the cooperativity domain is estimated to be on the order of 700 molecular units.[41] In addition, $(TMTSF)_2PF_6$ exhibits a rapidly changing (and strongly non-Arrhenius) relaxation time with probe energy in the kHz regime.[26] This behavior has been associated with the slowing down of the phason dynamics. Unfortunately, it is difficult to relate our microwave data to the low-frequency dielectric studies of Lasjaunias *et al.*[26] because the measurement frequencies are several decades apart. As discussed elsewhere,[23] the higher frequency measurements may be unrelated to the lower energy cooperative relaxation, as they provide a more local probe of the collective mode polarization. The dielectric response at 3.5 K can also be thought of in terms of collective mode pinning. In the weak pinning limit, the transverse Fukayama-Lee-Rice (FLR) length, L_T, characterizes the length scale over which the SDW is pinned.[59,60] As the "system viscosity" increases upon approach to T_g, the extent of the density wave undulations (as measured by L_T) decreases, leading to a drop in ϵ_1.

As shown in Fig. 10, there is a strong stabilization of the glassy phase with applied magnetic field.[24] Whereas the 3.5 K boundary does not move at low fields, it varies greatly above $\approx$ 0.5 T, suggesting that the length over which the density wave is pinned undergoes a fundamental change in the 0.5 T field regime. This effect may be related to the glassy domain structure below 3.5 K.[26]

We can gain a preliminary understanding of the magnetic-field dependence of the glassy (SDW 1→SDW 2) boundary within a model developed by Bjeliš and Maki[62] in which the field acts to reduce the effective transverse Fermi velocity, v_2, with direct consequences for *condensate* induced a–b plane orbital motion. Two important length scales emerge from the analysis.[62] The first is the transverse thermal coherence length, $\xi_{\rm th}$, which describes fluctuations of the order parameter near the transition temperature. The second is the transverse FLR coherence length, L_T, which defines a length scale over which the density wave is pinned. Because application of a magnetic field ($H \parallel c^*$) reduces the effective Fermi velocity, both $\xi_{th,b} \sim v_2^*/T \sim t_b/T$ and $L_T \sim (v_2^*/v_2)^2$ decrease with H.[62] Consequently, the fluctuations and spatial distortion of the phase (which must be overcome to achieve glassy cooperativity) are reduced with H.[62] Therefore, the glass transition temperature, which measures the energy scale for cooperativity, is expected to increase with applied field. That the SDW 1→SDW 2 boundary rises supralinearly with H (Fig. 10) seems to indicate a more important role for pinning considerations.

Despite the slowing down of phason dynamics at T_g, the dielectric response is not static at low temperature. We attribute the slight upturn in ϵ_1 near 1.9 K to the SDW 2 → SDW 3 transition. The magnetic-field effects here are weaker than at the 3.5 K glassy boundary. As shown in Fig. 10, the transition temperature increases slightly with applied field, reaching ≈6 K at 7 T. Although less is known about the SDW 2→SDW 3 transition, it is also associated with lattice specific heat and NMR anomalies in the PF_6 salt.[34,39] Our data are consistent with previous zero field results, but additional NMR data is clearly needed for comparison. The possibility that the 1.9 K feature is a secondary relaxation of the glassy structure should be examined in future work.

In addition to resolving the magnetic-field dependence of the aforementioned condensate boundaries, we observe preliminary evidence for a weak low-temperature/low-field region within SDW 2.[24] The 0.5 T structure does not seem to be *directly* related to the spin-flop transition due to the direction of the applied field (which is inconsistent with the magnetic susceptibility results[5]) and the limited temperature range of the boundary. Aside from noting that the approach to this phase seems to correlate with the appearance of a local maximum in σ_1 for both the AsF_6 and PF_6 samples, we have made little progress in understanding the specific nature of the low field regime. Due to the small sample size and the weak signal level of the 0.5 T boundary, the methods that can be brought to bare on this problem are limited.

V. CONCLUSION

We have reported the 16.5 GHz dielectric response of the quasi-one-dimensional Bechgaard salt $(TMTSF)_2AsF_6$ at temperatures above and below the 12 K antiferromagnetic phase transition as a function of external magnetic field. Data were collected with the magnetic field along the TMTSF chain direction as well as along the hard axis direction. These are the first microwave dielectric measurements that have been reported on the AsF_6 salt in the presence of a magnetic field.

In general, the response of the AsF_6 compound is in good agreement with results obtained for the PF_6 salt. In both cases, quasiparticle effects are important in the normal state and near the 12 K transition, whereas condensate effects dominate ϵ_1 and ϵ_2 well below T_c. Field and temperature sweeps concentrating in the 1.7–7 K and 0–3 T range have allowed us to construct an H–T diagram, which illustrates the complex behavior of the condensate at low temperatures and applied fields ($H \parallel c^*$). In addition to mapping out the behavior of the glassy (SDW 1→SDW 2) and SDW 2→SDW 3 boundaries in a magnetic field, these measurements seem to reveal a weak low-temperature/low-field phase within SDW 2. Comparing the condensate phase boundaries obtained from changes in ϵ_1 with previous NMR and specific heat results, we find good agreement. It is our hope that this work will stimulate further NMR investigations of the type reported in Ref. 31, which might be used to map out larger areas of the H-T diagram and characterize the various condensate regions.

ACKNOWLEDGMENTS

This work was supported by grants from the Natural Science and Engineering Research Council of Canada (NSERC) and the Fonds pour la Formation de Chercheurs et l'Aide à la Recherche (FCAR) of the Government of Québec. We greatly appreciate the technical assistance of M. Castonguay and C.D. Porter, helpful conversations with C. Bourbonnais and Y. Trudeau, and useful correspondence with G. Kriza.

*Current address: Department of Chemistry, State University of New York at Binghamton, Binghamton, NY 13902-6016.
[1] G. Grüner, Rev. Mod. Phys. **66**, 1 (1994).
[2] C. Bourbonnais, in Proceedings of the International School of Physics "Enrico Fermi," Course CVI, Current Trends in the Physics of Materials, edited by G.F. Chiarotti, F. Fumi, and M.P. Tosi (North-Holland, Amsterdam, 1990).
[3] T. Ishiguro and K. Yamaji, in *Organic Superconductors*, edited by P. Fulde, Springer Series of Solid State Sciences Vol. 88 (Springer-Verlag, Berlin, 1990).
[4] W. Kang, S.T. Hannahs, and P.M. Chaikin, Phys. Rev. Lett. **70**, 3091 (1993).
[5] K. Mortensen, Y. Tomkiewicz, and K. Bechgaard, Phys. Rev. B **25**, 3319 (1982).
[6] C. Gaonach and G. Creuzet, Synth. Met. **16**, 299 (1986).
[7] G. Creuzet, C. Gaonach, and B. Hamzic, Synth. Met. **19**, 245 (1987).
[8] G. Grüner, Rev. Mod. Phys. **60**, 1129 (1988).
[9] A.J. Heeger, S. Kivelson, J.R. Schrieffer, and W.-P. Su, Rev. Mod. Phys. **60**, 782 (1988).
[10] J.W. Bray, L.V. Interrante, I.S. Jacobs, and J.C. Bonner, in *Extended Linear Chain Compounds*, edited by J.S. Miller (Plenum, New York, 1983), Vol. 3.
[11] S. Donovan, Y. Kim, L. Degiorgi, M. Dressel, and G. Grüner, Phys. Rev. B. **49**, 3363 (1994).
[12] S. Donovan, Y. Kim, L. Degiogi, and G. Grüner, J. Phys. (France) **3**, 1493 (1993).
[13] K. Kornelsen, J.E. Eldridge, and G.S. Bates, Phys. Rev. B **35**, 9162 (1987).
[14] C.S. Jacobsen, D.B. Tanner, and K. Bechgaard, Phys. Rev. B **28**, 7019 (1983).
[15] D. Quinlivan, Y. Kim, G. Grüner, and F. Wudl, Phys. Rev. Lett. **65**, 1816 (1990).
[16] S. Donovan, L. Degiorgi, and G. Grüner, Europhys. Lett. **19**, 433 (1992).
[17] H.H.S. Javadi, S. Sridhar, G. Grüner, L. Chiang, and F. Wudl, Phys. Rev. Lett. **55**, 1216 (1985).
[18] A. Jánossy, M. Hardiman, and G. Grüner, Solid State Commun. **46**, 21 (1983).
[19] A. Zettl, G. Grüner, and E.M. Engler, Phys. Rev. B. **25**, 1443 (1982).
[20] S. Donovan, O. Klein, M. Dressel, K. Holczer, and G. Grüner, Int. J. Infrared Millimeter Waves **14**, 2459 (1993).
[21] M. Dressel, O. Klein, S. Donovan, and G. Grüner, Int. J. Infrared Millimeter Waves **14**, 2489 (1993).
[22] P.A. Lee, T.M. Rice, and P.W. Anderson, Solid State Commun. **14**, 703 (1974).
[23] J.L. Musfeldt, M. Poirier, P. Batail, and C. Lenoir, Phys. Rev. B **51**, 8347 (1995).
[24] J.L. Musfeldt, M. Poirier, P. Batail, and C. Lenoir, Europhys. Lett. **30**, 105 (1995).
[25] G. Mihály, Y. Kim, and G. Grüner, Phys. Rev. Lett. **66**, 2806 (1991).
[26] J.C. Lasjaunias, K. Biljakovic, F. Nad, P. Monceau, and K. Bechgaard, Phys. Rev. Lett. **72**, 1283 (1994).
[27] O. Traetteberg, G. Kriza, C. Lenoir, Y.-S. Huang, P. Batail, and D. Jérome, Synth. Met. **55–57**, 2785 (1993).
[28] O. Traetteberg, G. Kriza, C. Lenoir, Y.-S. Huang, P. Batail, and D. Jérome, Phys. Rev. B **49**, 409 (1994).
[29] W.H. Wong, M.E. Hanson, W.G. Clark, B. Alavi, and G. Grüner, Phys. Rev. Lett. **72**, 2640 (1994).
[30] E. Barthel, G. Quirion, P. Wzietek, D. Jérome, J.B. Christiansen, M. Jorgensen, and K. Bechgaard, Phys. Rev. Lett. **71**, 2825 (1993).
[31] W.G. Clark, M.E. Hanson, W.H. Wong, and B. Alavi, J. Phys. (France) IV **3**, 235 (1993).
[32] W.H. Wong, M.E. Hanson, B. Alavi, W.G. Clark, and W.A. Hines, Phys. Rev. Lett. **70**, 1882 (1993).
[33] E. Barthel, G. Quirion, P. Wzietek, D. Jérome, J.B. Christiansen, M. Jorgensen, and K. Bechgaard, Europhys. Lett. **21**, 87 (1993).
[34] T. Takahashi, T. Harada, Y. Kobayashi, K. Suzuki, K. Murata, and G. Saito, Synth. Met. **41-43**, 3985 (1991).
[35] T. Takahashi, Y. Maniwa, H. Kaqamura, and G. Saito, J. Phys. Soc. Jpn. **55**, 1364 (1986).
[36] C. Bourbonnais, P. Stein, D. Jérome, and A. Moradpour, Phys. Rev. B **33**, 7608 (1986).
[37] J.M. Delrieu, M. Roger, Z. Toffano, A. Moradpour, and K. Bechgaard, J. Phys. (Paris) **47**, 839 (1986).
[38] J. Coroneus, B. Alavi, and S.E. Brown, Phys. Rev. Lett. **70**, 2332 (1993).
[39] J.C. Lasjaunias, K. Biljakovic, P. Monceau, and K. Bechgaard, Solid State. Commun., **84**, 297 (1992).
[40] S.E. Brown, B. Alavi, G. Grüner, and K. Bartholomew, Phys. Rev. B **46**, 10 483 (1992).
[41] J. Odin, J.C. Lasjaunias, K. Biljaković, P. Monceau, and K. Bechgaard, Solid State Commun. **91**, 523 (1994).
[42] M. Nagasawa, T. Sambongi, K. Nomura, and H. Anzai, Solid State Commun. **93**, 33 (1995).
[43] J.P. Ulmet, A. Khmou, and L. Bachere, Synth. Met. **19**, 271 (1987).
[44] G. Kriza, G. Quirion, O. Traetteberg, and D. Jérome, Europhys. Lett. **16**, 585 (1991).
[45] J.C. Scott, H.J. Pederson, and K. Bechgaard, Phys. Rev. Lett. **45**, 2125 (1980).
[46] L.I. Buranov and I.F. Shchegolev, Instrum. Exp. Tech. **14**, 528 (1971).
[47] O. Klein, S. Donovan, M. Dressel, and G. Grüner, Int. J. Infrared Millimeter Waves **14**, 2423 (1993).
[48] Y.M. Kim, R. Gaál, B. Alavi, and G. Grüner, Phys. Rev. B **50**, 13 867 (1994).
[49] O. Traetteberg, L. Balicas, and G. Kriza, J. Phys. (France) IV **3**, 61 (1993).
[50] It is important to note that ϵ_1 is not a true thermodynamic quantity, and therefore not related to a phase transition in an *a priori* way. However, when correlated with thermodynamic measurements, changes in ϵ_1 can provide an excellent indication for a phase boundary. That changes in thermodynamic properties occur at these temperatures (Refs. 39 and 38) provides support for our method.
[51] O. Traetteberg, Doctoral thesis, Université de Paris-Sud, 1993.
[52] K. Yamaji, J. Phys. Soc. Jpn. **51**, 2787 (1982).
[53] K. Yamaji, J. Phys. Soc. Jpn. **53**, 2189 (1984).
[54] K. Yamaji, J. Phys. Soc. Jpn. **54**, 1034 (1985).
[55] K. Yamaji, Synth. Met. **13**, 29 (1986).
[56] G. Montambaux, Phys. Rev. B **38**, 4788 (1988).
[57] N.W. Ashcroft and D.D. Mermin, in *Solid State Physics*, edited by D. G. Crane (Saunders College, Philadelphia, 1976).
[58] K. Maki and A. Virosztek, Phys. Rev. B **42**, 655 (1990).
[59] H. Fukuyama and P.A. Lee, Phys. Rev. B **17**, 535 (1978).
[60] P.A. Lee and T.M. Rice, Phys. Rev. B **19**, 3970 (1979).
[61] G. Adam and J.H. Gibbs, J. Chem. Phys. **43**, 139 (1965).
[62] A. Bjelis and K. Maki, Phys. Rev. B **44**, 6799 (1991).